

Experimental study on post-buckled composite single-stringer specimens with initial delamination under fatigue loads

Raimondo, A.; Paz Mendez, J.; Bisagni, C.

Publication date

2021

Document Version

Final published version

Published in

Proceedings of the American Society for Composites, Thirty-Sixth Technical Conference

Citation (APA)

Raimondo, A., Paz Mendez, J., & Bisagni, C. (2021). Experimental study on post-buckled composite single-stringer specimens with initial delamination under fatigue loads. In *Proceedings of the American Society for Composites, Thirty-Sixth Technical Conference* (pp. 418-428)

Important note

To cite this publication, please use the final published version (if applicable).
Please check the document version above.

Copyright

Other than for strictly personal use, it is not permitted to download, forward or distribute the text or part of it, without the consent of the author(s) and/or copyright holder(s), unless the work is under an open content license such as Creative Commons.

Takedown policy

Please contact us and provide details if you believe this document breaches copyrights.
We will remove access to the work immediately and investigate your claim.

Experimental Study on Post-Buckled Composite Single-Stringer Specimens with Initial Delamination under Fatigue Loads

ANTONIO RAIMONDO, JAVIER PAZ MENDEZ
and CHIARA BISAGNI

ABSTRACT

The fatigue damage tolerance of a composite stiffened structure in post-buckling conditions is experimentally investigated in this work. Single-stringer specimens with an initial delamination, artificially created during the manufacturing process, are tested under cyclic compressive load. Six nominally identical specimens are manufactured: two tested under quasi-static load to understand the compressive behavior of the structure and four under fatigue load cycling between pre- and post-buckling conditions at two different maximum loads. During the tests, digital image correlation system and ultrasonic C-scan are adopted to follow the evolution of the out-of-plane displacements and the propagation of the delamination. Depending on the load level, the delamination starts to grow already in the first cycle or after a few thousand cycles, but in both cases the propagation is fast at the beginning, then slows down gradually. The fatigue tests are interrupted after 150,000 cycles and the specimens are subjected to quasi-static compressive load to evaluate the residual strength of the structure.

INTRODUCTION

In the modern aeronautical industry, composite stiffened panels are one of the most common types of structural component. This type of structure is usually able to sustain loads higher than the buckling load without any permanent deformation. However, the application of post-buckling design in the aeronautical sector has not yet been exploited, due to the difficulties in predicting damage initiation and propagation. In particular, under fatigue loading conditions, the interaction between large displacements, high local stress and the accumulation of cyclic damage may cause the separation of the skin from the stringer at the interface [1-2]. Fatigue-driven delamination represents one of the most critical types of damage, since it is difficult to detect and can rapidly growth under service loading conditions.

Delft University of Technology, Faculty of Aerospace Engineering, Kluyverweg 1, 2629 HS Delft, the Netherlands.

Allowing composite stiffened panels to operate in post-buckling regime would enable the exploration of innovative design solutions resulting in a weight reduction without compromising the load carrying capability of the structure.

Despite the large number of studies on this topic, the prediction of fatigue-driven delamination in aerospace composite structures represents still an open issue, since the applicability of the available numerical techniques is mainly limited to coupon specimens [3-6]. Furthermore, only few experimental tests are reported in literature on stiffened composite structures in post-buckling regime, due to the high costs for the manufacturing and the difficulties in terms of time and complexity in performing this type of test [7-9].

An experimental test campaign has been carried out in [10-12] on the evolution of an initial delamination on a single-stringer specimen subjected to a cyclic compressive load with the structure oscillating between pre- and post-buckling conditions.

The single-stringer specimen has been designed to have a small size and low manufacturing costs while still maintaining a structural complexity similar to a multi-stringer panel in terms of damage mechanisms. Because of its limited size, the specimen can be analyzed to validate numerical models without requiring unreasonable computational costs.

In this work, an experimental test campaign is performed on single-stringer composite specimens with an initial delamination, artificially created by inserting a Teflon film between the skin and the stringer during the manufacturing, subjected to fatigue compressive loads between pre- and post-buckling conditions at different load levels. The objective is to understand the effect of the maximum load on the propagation of the delamination and on the fatigue life of the component and to provide experimental data to validate numerical techniques.

After the manufacturing process, the first two specimens are tested under compressive quasi-static loads up to the complete failure. Then, four specimens are tested under compressive fatigue loads at two different load levels. Three-dimensional digital image correlation systems are used to monitoring the out-of-plane displacements and the evolution of the post-buckling shape, while ultrasonic C-scans are performed to track the progression of the delamination front. After 150,000 cycles the specimens are quasi-statically loaded until failure to evaluate the residual strengths.

EXPERIMENTAL TESTING

The Single-Stringer Compressive Specimen (SSCS) was developed in [1] with the aim to investigate the post-buckling response of composite stiffened panels. The specimen exhibits the structural complexity of a multi-stringer panel despite its limited size, making the SSCS ideal as a benchmark for the validation of numerical methodologies.

In total 6 nominally identical specimens were manufactured. At first, two of the specimens are tested quasi-statically to understand the behavior of the structure in terms of maximum load, buckling load and post-buckling deformation shapes, then, based on the results of the quasi-static tests, the remaining specimens are tested under fatigue loads between pre- and post-buckling conditions at two different load levels.

The specimens with their labels and the type of test performed are summarized in Table I.

TABLE I. SINGLE-STRINGER TEST MATRIX.

Specimen	Type of test
SSCS1-2	Quasi-Static
SSCS3-6	Fatigue

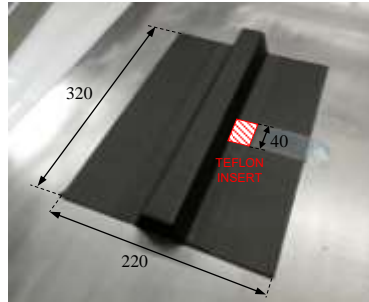


Figure 1. Single-stringer specimen geometry.

Specimen Description

The single-stringer specimen consists of a flat skin panel co-cured with an omega stringer. The total length of the specimen is 320 mm with a free length of 260 mm, considering 30 mm tabs at each end. The initial delamination of 40 mm is artificially created by inserting a Teflon film between the skin and the stringer during the manufacturing before the curing process. The geometrical characteristics of the specimen are displayed in Figure 1.

The specimen is made of IM7/8552 carbon-epoxy tape with the skin composed of an 8-ply quasi-isotropic laminate with the stacking sequence $[45/90/-45/0]_s$, while the stringer has 7 plies with the layup $[-45/0/45/0/45/0/-45]$. The nominal ply thickness is 0.125 mm. After the curing process both ends of the specimen are encased in 30 mm tabs made of metal filled casting resin RenCast® CW 2418-1 hardened with Ren® HY 5160-1 to ensure that the compressive load is applied uniformly. An image of the specimens with the end tabs before the testing is shown in Figure 2.



Figure 2. Single-stringer specimens before the test.

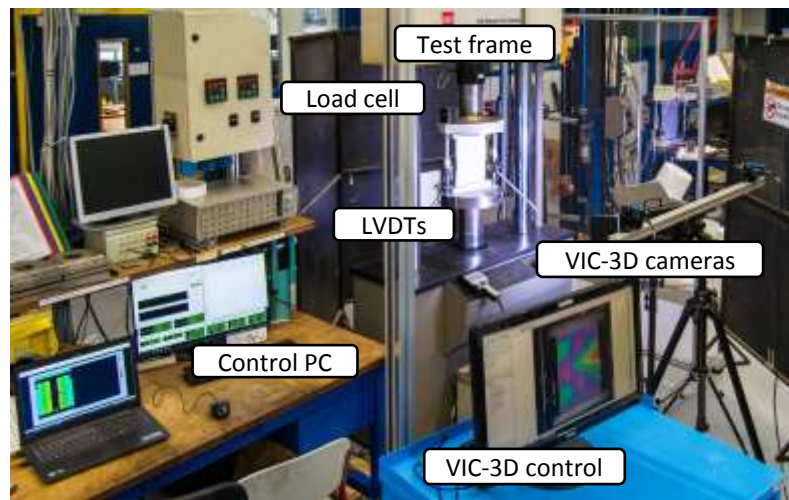


Figure 3. Test set-up.

Test Set-up

An MTS servo-hydraulic testing machine with a load cell of 500 kN is adopted for all the tests. The general set-up employed for the quasi-static and fatigue experiments is shown in Figure 3.

The end-shortening is measured using two linear variable displacement transducers (LVDT) positioned on the opposite sides of the specimens to detect any load misalignment during the tests.

A digital image correlation system is adopted to evaluate the out-of-plane displacements, the deformation fields, and to monitor the buckling and post-buckling shapes of the specimen during the test as the delamination propagates. For all the tests, a three-dimensional VIC-3D system is employed pointing at the back of the specimen from the skin side.

An ultrasonic C-scan system is used to track the progression of the delamination. The specimen is removed from the machine and placed in a water tank where it is automatically fully scanned with an Olympus Epoch® 650 Ultrasonic Flaw Detector. An overview of the C-scan apparatus is shown in Figure 4.

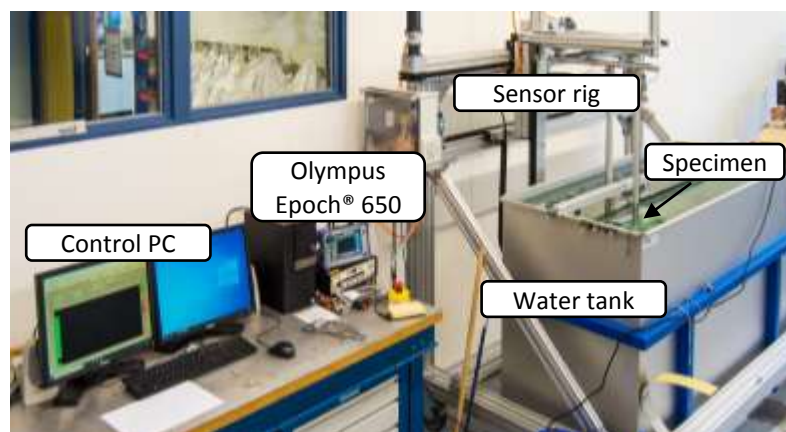


Figure 4. C-scan apparatus.

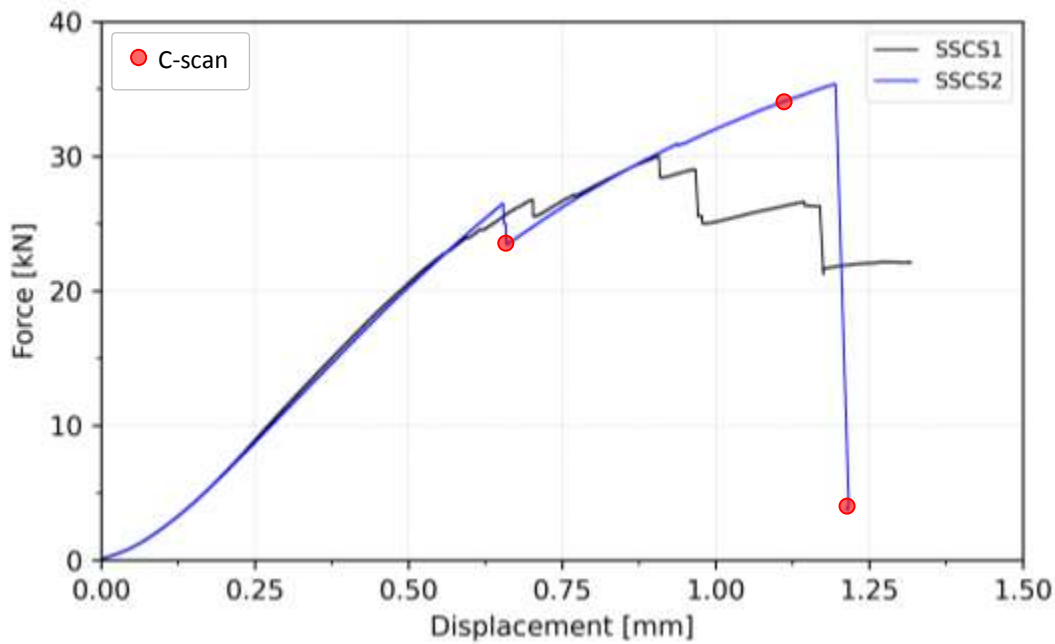


Figure 5. Force-displacement response for the quasi-static tests.

QUASI-STATIC TESTS

The specimens SS-CS1 and SS-CS2 are subjected to quasi-static compressive load under displacement-controlled conditions with a loading rate of 0.01 mm/min. The SS-CS1 specimen is tested in one single run until the global failure of the structure while the SS-CS2 test is divided in 3 different runs. At the end of each run the specimen is taken out of the machine to perform the ultrasonic C-scan and evaluate the extension of the delamination. The results in term of load as function of the applied displacement for the quasi-static tests are reported in Figure 5.

After an initial linear behavior, the global buckling of the specimen starts in the skin with three half-waves on the side of the delamination and two on the opposite side. The transition into post-buckling is gradual so the buckling load cannot be precisely identified, although a value of 15 kN can be estimated. A sudden opening of the delamination occurs at an applied load of 26.5 kN, as can be observed from the load drop in both the curves in the graph shown in Figure 5. The opening of the delamination causes a change in the post-buckling shape with one half-wave on the delamination side and three half-waves on the opposite side. As the compressive load increases, the delamination slowly grows until it starts to propagate under the opposite stringer flange. After this point, the delamination suddenly extends to the other side of the specimen causing the complete separation of the skin from the stringer and creating a tunnel under the stringer which results in the global collapse of the specimen at an applied load of 35.4 kN for the specimen SS-CS2.

The behavior of both specimens, SS-CS1 and SS-CS2, is highly consistent in terms of pre- and post-buckling stiffness and delamination buckling load. However, the final failure of the specimen SS-CS1 occurred at a much lower load, 30.0 kN, with a different failure mode with a breakage in the skin, most likely caused by a

misalignment between the loading surfaces. The failure mode of SSCS2 described above is more representative

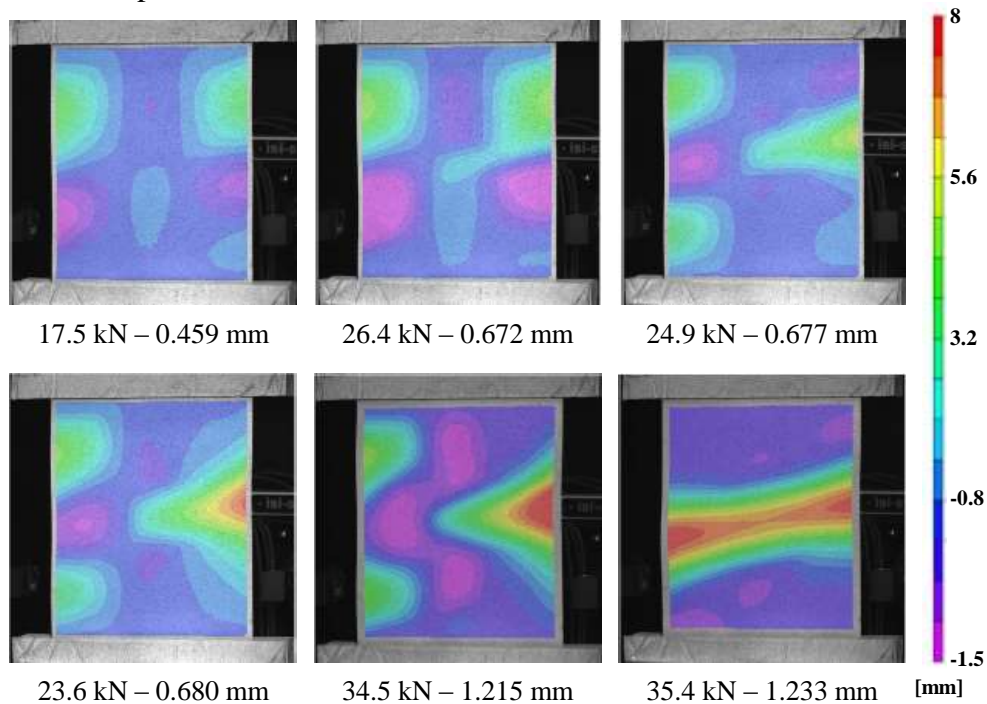


Figure 6. Out-of-plane displacements of the skin during the quasi-static test (SSCS2).

of the collapse of this type of specimen when subjected to compressive loads, as previous experimental campaigns have demonstrated [12].

The sequence of events leading to the failure of the specimen SSCS2 can be appreciated in Figure 6, where the out-of-plane displacements measured with the VIC-3D system are reported at different values of the compressive load and applied displacement.

The quasi-static test of SSCS2 has been interrupted twice before the global failure to evaluate the extension of the delamination. The images from the ultrasonic C-scan before the test, after the local buckling of the delamination, when the delamination reaches the opposite stringer flange and, finally, after the final failure, are reported in Figure 7.

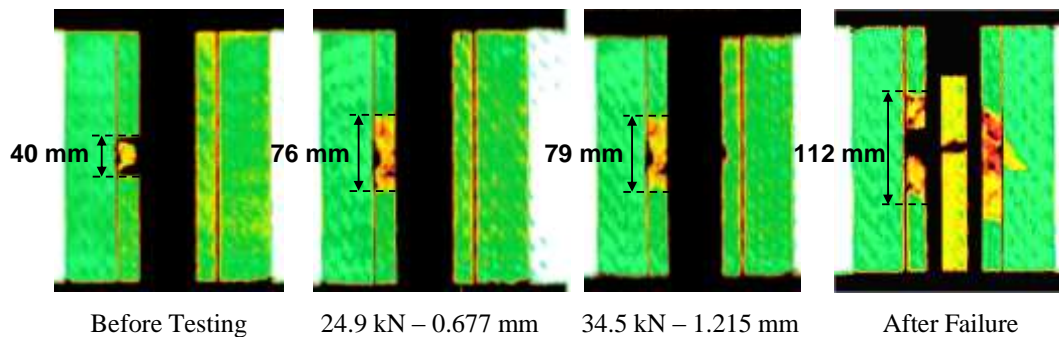


Figure 7. Delamination propagation measured with ultrasonic C-scan (SSCS2).

TABLE II. SINGLE-STRINGER FATIGUE TESTS.

Specimen	Maximum Load (% of the delamination buckling load)	Minimum Load
SSCS3-4	25.2 kN (95%)	2.52 kN
SSCS5-6	27.1 kN (102.5%)	2.71 kN

FATIGUE TESTS

The specimens from SSCS3 to SSCS6 are tested under cyclic load with a load ratio of $R = 0.1$ and a frequency of 2 Hz. Images are captured by the digital image correlation system every 250 cycles at the minimum and at the maximum load to monitor the out-of-plane displacements, allowing the early detection of any propagation of the delamination. Based on the results from the quasi-static tests, two different maximum loads are selected: 25.2 kN and 27.1 kN corresponding to 95% and 102.5% of the delamination buckling load (26.5 kN), respectively. The aim is to analyze the fatigue behavior of the SSCS specimens at two different maximum loads, before and after the local buckling of the delamination.

Two specimens are tested for each load level. The performed tests and the applied loads are summarized in Table II.

During the test, the specimens are removed from the machine and inspected with ultrasonic C-scan at regular interval or when a sudden growth of the delamination is evident from the VIC3D or from visual inspection.

For all the performed fatigue tests, no global failure occurred. The specimens were able to sustain 150,000 cycles, which is a value higher than the number of cycles that an aeronautical component is expected to withstand between two inspection intervals. For this reason, after reaching 150,000 cycles the specimens are subjected to quasi-static load until the global failure to evaluate the residual strength.

In Figure 8 and Figure 9, the out-of-plane displacements measured with the VIC3D at different value of the number of cycles are reported for the specimens SSCS3 and SSCS5, respectively.

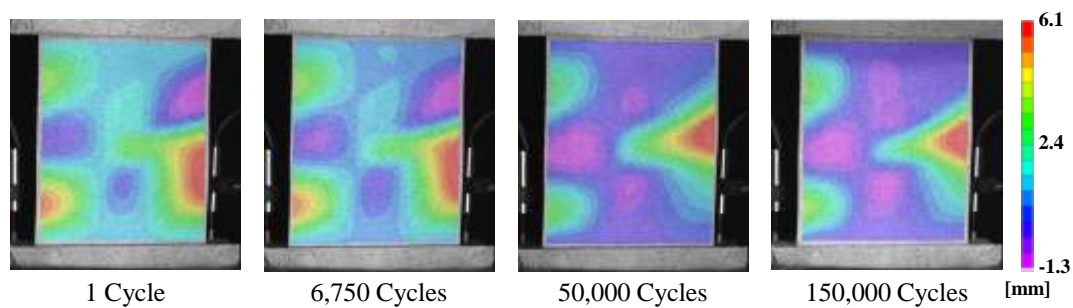


Figure 8. Out-of-plane displacements of the skin during the fatigue test (SSCS3).

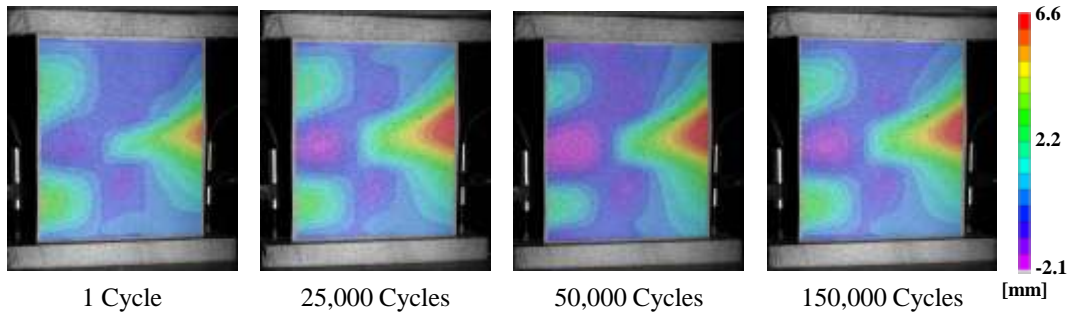


Figure 9. Out-of-plane displacements of the skin during the fatigue test (SSCS5).

For the specimen SSCS5, the propagation of the delamination starts on the first cycle, since the maximum load is higher than the buckling load of the delamination. On the other hand, for the specimen SSCS3 the propagation is gradual and affects the global buckling shape of the structure, which exhibits the same sequence of events already observed in the quasi-static tests and shown in Figure 6.

Images from the ultrasonic C-scan at different number of cycles are reported in Figure 10 and 11 for the specimens SSCS3 and SSCS5, respectively.

The delamination front for all the performed tests exhibits a rounded shape with a more extended propagation on the sides compared to the center.

The extension of the delamination as function of the number of cycles is compared for all the performed tests in Figure 12. The opening size is reported as the average between the measurements taken at the center, and at the left and right sides of the delamination.

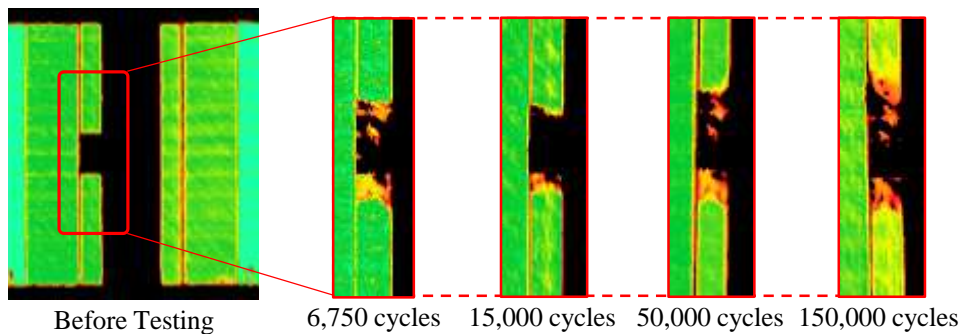


Figure 10. Ultrasonic C-scan at different fatigue cycles (SSCS3).

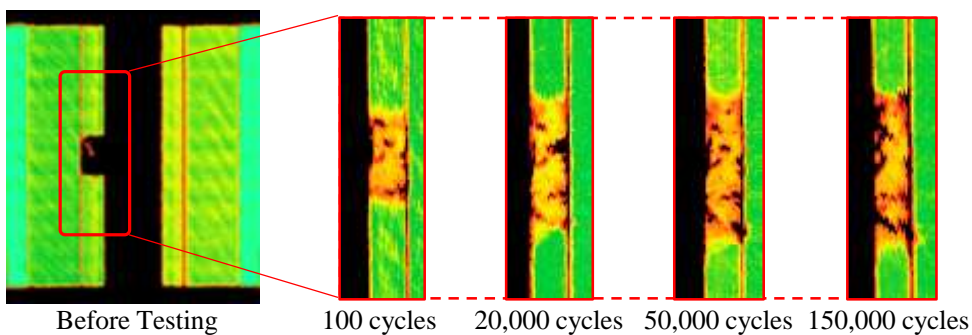


Figure 11. Ultrasonic C-scan at different fatigue cycles (SSCS5).

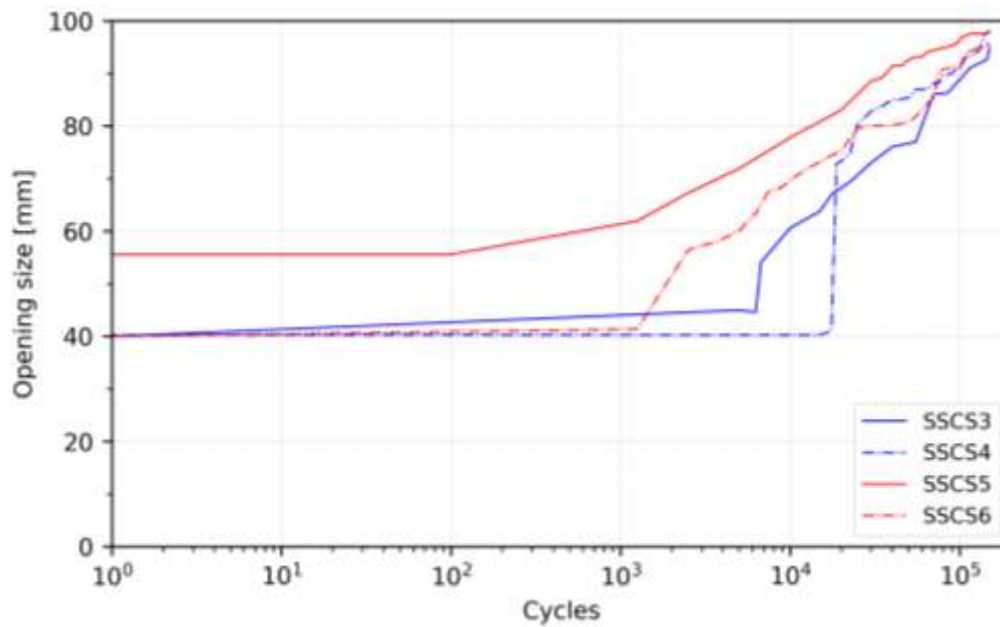


Figure 12. Delamination opening size with the number of fatigue cycles.

For all the fatigue test, the propagation of the delamination is fast at the beginning, then slows down gradually, as can be observed from the nearly linear trends in the semi-logarithmic graph in Figure 12. As expected, the size of the delamination is larger on average for the specimens SSCS5 and SSCS6 compared with the specimens SSCS3 and SSCS3 at equal number of cycles due to the higher maximum load. However, for all the tests the delamination length stabilizes around a value of 100 mm.

After 150,000 cycles the specimens are subjected to a quasi-static compressive load until the failure. The values of the residual strength are reported for all the quasi-static and fatigue test in Table III.

The average residual strength is 31.9 kN which represents approximately 90% of the quasi-static failure of specimen SSCS2. The failure mode of all the specimens is very consistent as it can be appreciated in Figure 13, where images of the specimens captured after the failure are reported.

TABLE III. SINGLE-STRINGER SPECIMENS STRENGTH.

Specimen	Test	Maximum Load (Fatigue)	Strength
SSCS1	Quasi-static	//	30.0 kN
SSCS2	Quasi-static	//	35.4 kN
SSCS3	Fatigue	25.2 kN	32.1 kN
SSCS4	Fatigue	25.2 kN	33.2 kN
SSCS5	Fatigue	27.1 kN	32.9 kN
SSCS6	Fatigue	27.1 kN	29.7 kN

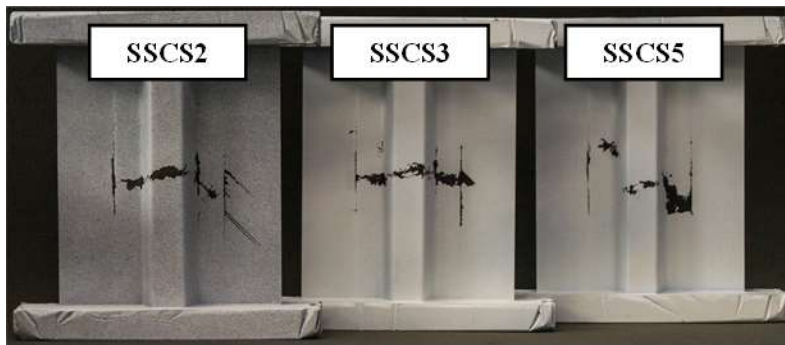


Figure 13. Images of the specimens after failure.

CONCLUSIONS

An experimental test campaign has been carried out on Single-Stringer Compression Specimens (SSCS) under quasi-static and fatigue loading conditions. Six nominally identical specimens have been manufactured with an initial artificial delamination of 40 mm positioned between the skin and the stringer during the manufacturing. Two specimens have been tested under quasi-static load and four under fatigue by cycling between pre-and post-buckling conditions. Digital image correlation and ultrasonic C-scan have been adopted to monitor the out-of-plane displacements and the growth of the delamination during all the tests.

Based on the results of the quasi-static tests two different load level have been selected for the fatigue tests: before and after the buckling of the delamination. The fatigue behavior has been consistent for all the specimens. After an initial rapid propagation, the growth of the delamination gradually slows down, stabilizing around a length of 100 mm. After 150,000 cycles, the specimens have been tested under quasi-static load resulting in a residual strength of approximately 90% of the quasi-static strength.

The results presented in this work contribute to a better understanding of the post-buckling fatigue phenomenon and provide invaluable experimental data for the validation of numerical models.

ACKNOWLEDGMENTS

This work is sponsored by the Office of Naval Research (ONR), under grant award number N62909-17-1-2129. The views and conclusions contained herein are those of the authors only and should not be interpreted as representing those of ONR, the U.S. Navy or the U.S. Government.

REFERENCES

1. Bisagni, C., R. Vescovini, and C.G. Dávila. 2011. "Development of a Single-stringer Compression Specimen for the Assessment of Damage Tolerance of Postbuckled Structures," *Journal of Aircraft*, 48(2):495–502.

2. Anyfantis, K.N., N.G. Tsouvalis. 2012. "Post Buckling Progressive Failure Analysis of Composite Laminated Stiffened Panels," *Applied Composite Materials*, 19(3-4):219-236.
3. Turon, A., J. Costa, P.P. Camanho and C.G. Dávila. 2007. "Simulation of Delamination in Composites Under High-cycle Fatigue," *Composites Part A: Applied Science and Manufacturing*, 38(11):2270-2282.
4. Raimondo A., and C Bisagni. 2019. "Analysis of Local Stress Ratio for Delamination in Composites Under Fatigue Loads," *AIAA Journal*, 58(1).
5. Raimondo, A., and C. Bisagni. 2020. "Fatigue Analysis of a Post-buckled Composite Single-stringer Specimen Taking into Account the Local Stress Ratio," *Composite Part B: Engineering*, 193.
6. Dávila C.G. 2020. "From S-N to the Paris Law with a New Mixed-mode Cohesive Fatigue Model for Delamination in Composites," *Theoretical and Applied Fracture Mechanics*, 106.
7. Agarwal, B.L. 1982. "Postbuckling Behavior of Composite-stiffened-curved Panels Loaded in Compression—an Experimental Evaluation of Static and Fatigue Behavior of Graphite/Epoxy Curved Hat-stiffened Compression Panels Loaded Well Beyond Initial Buckling," *Exp. Mech.*, 22(6):231–6.
8. Abramovich H., and T. Weller. 2012. "Repeated Buckling and Postbuckling Behavior of Laminated Stringer Stiffened Composite Panels With and Without Damage," *Int. J. Struct. Stab. Dyn.*, 4:807–825.
9. Cordisco P., and C. Bisagni. 2011. "Cyclic Buckling Tests Under Combined Loading on Pre-Damaged Composite Stiffened Boxes," *AIAA Journal*, 49(8):1795–1807.
10. Bisagni C., and C.G. Dávila. 2014. "Experimental Investigation of the Postbuckling Response and Collapse of a Single-Stringer Specimen," *Composite Structures*, 108:493-503.
11. Davila C.G., and C. Bisagni. 2018. "Fatigue Life and Damage Tolerance of Postbuckled Composite Stiffened Structures with Indentation Damage," *Journal of Composite Materials*, 52(7):931–943.
12. Dávila C.G., and C. Bisagni. 2017. "Fatigue Life and Damage Tolerance of Postbuckled Composite Stiffened Structures with Initial Delamination," *Composite Structures*, 131:73-84.